

Accepted Manuscript

Title: CT Coronary Calcium Scoring with Tin Filtration Using Iterative Beam-Hardening Calcium Correction Reconstruction

Authors: Christian Tesche, Carlo N. De Cecco, U. Joseph Schoepf, Taylor M. Duguay, Moritz H. Albrecht, Domenico De Santis, Akos Varga-Szemes, Virginia W. Lesslie, Ullrich Ebersberger, Richard R. Bayer, Christian Canstein, Ellen Hoffmann, Thomas Allmendinger, John W. Nance



PII: S0720-048X(17)30111-0
DOI: <http://dx.doi.org/doi:10.1016/j.ejrad.2017.03.011>
Reference: EURR 7777

To appear in: *European Journal of Radiology*

Received date: 22-12-2016
Accepted date: 21-3-2017

Please cite this article as: Tesche Christian, De Cecco Carlo N, Schoepf U Joseph, Duguay Taylor M, Albrecht Moritz H, De Santis Domenico, Varga-Szemes Akos, Lesslie Virginia W, Ebersberger Ullrich, Bayer Richard R, Canstein Christian, Hoffmann Ellen, Allmendinger Thomas, Nance John W. CT Coronary Calcium Scoring with Tin Filtration Using Iterative Beam-Hardening Calcium Correction Reconstruction. *European Journal of Radiology* <http://dx.doi.org/10.1016/j.ejrad.2017.03.011>

This is a PDF file of an unedited manuscript that has been accepted for publication. As a service to our customers we are providing this early version of the manuscript. The manuscript will undergo copyediting, typesetting, and review of the resulting proof before it is published in its final form. Please note that during the production process errors may be discovered which could affect the content, and all legal disclaimers that apply to the journal pertain.

Original Research – Cardiac Imaging

CT Coronary Calcium Scoring with Tin Filtration Using Iterative Beam-Hardening Calcium Correction Reconstruction

Christian Tesche, MD^{a,b}; Carlo N. De Cecco, MD, PhD^a; U. Joseph Schoepf, MD^{a,e};
Taylor M. Duguay, BS^a; Moritz H. Albrecht, MD^{a,c}; Domenico De Santis, MD^{a,d};
Akos Varga-Szemes, MD, PhD^a; Virginia W. Lesslie, BS^a; Ullrich Ebersberger, MD^{a,b};
Richard R. Bayer 2nd, MD^e; Christian Canstein, MSc^f; Ellen Hoffmann, MD^b;
Thomas Allmendinger, PhD^f; John W. Nance, MD^a

^aDivision of Cardiovascular Imaging, Department of Radiology and Radiological Science, Medical University of South Carolina, 25 Courtenay Drive, Charleston, SC, 29403, USA; tesche@musc.edu, nancej@musc.edu, dececco@musc.edu, albreco@musc.edu, domenico.desantis@hotmail.it, dcaruso85@gmail.com, vargaasz@musc.edu, duguay@musc.edu, lesslie@musc.edu, ebersberger@gmx.net, schoepf@musc.edu

^bDepartment of Cardiology and Intensive Care Medicine, Heart Center Munich-Bogenhausen, Engschalkinger Strasse 77, 81925 Munich, Germany; med1.kb@klinikum-muenchen.de

^cDepartment of Diagnostic and Interventional Radiology, University Hospital Frankfurt, Theodor-Stern-Kai 7, 60590 Frankfurt, Germany

^dDepartment of Radiological Sciences, Oncology and Pathology, University of Rome “Sapienza”, Piazzale Aldo Moro 5, 00185 Rome, Italy

^eDivision of Cardiology, Department of Medicine, Medical University of South Carolina, 25 Courtenay Drive, Charleston, SC, 29403, USA; bayer@musc.edu

^fComputed Tomography - Research & Development, Siemens Healthcare GmbH, Forchheim, Germany; Siemensstrasse 1, 91301 Forchheim, Germany; christian.canstein@siemens.com, thomas.allmendinger@siemens.com

Corresponding Author:

U. Joseph Schoepf, MD
Heart & Vascular Center
Medical University of South Carolina
Ashley River Tower
25 Courtenay Drive
Charleston, SC 29425-2260, USA
Phone: +1-843-876-7146
Fax: +1-843-876-3157
E-Mail: schoepf@musc.edu

Highlights

- CT coronary calcium scoring with tin filtration reduces radiation dose by 75%.
- IBHC CACS material reconstruction algorithm restores calcium values.
- There is excellent correlation between IBHC Sn100kVp scans and 120kVp acquisitions.
- Perfect agreement regarding Agatston score categories and cardiac risk categorization is found.
- The use of IBHC CACS reconstruction resulted in a cardiac risk reclassification of 1.6%.

Abstract

Objectives: To investigate the diagnostic accuracy of CT coronary artery calcium scoring (CACS) with tin pre-filtration (Sn100kVp) using iterative beam-hardening correction (IBHC) calcium material reconstruction compared to the standard 120kVp acquisition.

Background: Third generation dual-source CT (DSCT) CACS with Sn100kVp acquisition allows significant dose reduction. However, the Sn100kVp spectrum is harder with lower contrast compared to 120kVp, resulting in lower calcium score values. Sn100kVp spectral correction using IBHC-based calcium material reconstruction may restore comparable calcium values.

Methods: Image data of 62 patients (56% male, age 63.9 ± 9.2 years) who underwent a clinically-indicated CACS acquisition using the standard 120kVp protocol and an additional Sn100kVp CACS scan as part of a research study were retrospectively analyzed. Datasets of the Sn100kVp scans were reconstructed using a dedicated spectral IBHC CACS reconstruction to restore the spectral response of 120kVp spectra. Agatston scores were derived from 120kVp and IBHC reconstructed Sn100kVp studies. Pearson's correlation coefficient was assessed and Agatston score categories and percentile-based risk categorization were compared.

Results: Median Agatston scores derived from IBHC Sn100kVp scans and 120kVp acquisition were 31.7 and 34.1, respectively ($p=0.057$). Pearson's correlation coefficient showed excellent correlation between the acquisitions ($r=0.99$, $p<0.0001$). Agatston score categories and percentile-based cardiac risk categories showed excellent agreement ($\kappa=1.00$ and $\kappa=0.99$), resulting in a low cardiac risk reclassification of 1.6% with the use of IBHC CACS reconstruction. Image noise was 24.9 ± 3.6 HU in IBHC Sn100kVp and 17.1 ± 3.9 HU in 120kVp scans ($p<0.0001$). The dose-length-product was 13.2 ± 3.4 mGy*cm with IBHC Sn100kVp and 59.1 ± 22.9 mGy*cm with 120kVp scans ($p<0.0001$), resulting in a significantly lower effective radiation dose (0.19 ± 0.07 mSv vs. 0.83 ± 0.33 mSv, $p<0.0001$) for IBHC Sn100kVp scans.

Conclusion: Low voltage CACS with tin filtration using a dedicated IBHC CACS material reconstruction algorithm shows excellent correlation and agreement with the standard 120kVp acquisition regarding Agatston score and cardiac risk categorization, while radiation dose is significantly reduced by 75% to the level of a chest x-ray.

Abbreviations

BMI:	Body mass index
CACS:	Coronary artery calcium scoring
CAD:	Coronary artery disease
CCTA:	Coronary CT angiography
CI:	Confidence interval
CTDI _{vol} :	Volumetric CT dose index
DLP:	Dose-length-product
DSCT:	Dual-source CT
ED:	Effective dose
FBP:	Filtered-back-projection
HU:	Hounsfield units
IBHC:	Iterative beam hardening correction
SD:	Standard deviation

Keywords: Coronary artery disease, coronary artery calcium score, coronary computed tomographic angiography, tin filtration

Introduction

CT coronary artery calcium scoring (CACS) is a well-established screening test to assess cardiovascular risk and to guide the aggressiveness of prevention [1, 2]. The test is typically performed in *a priori* healthy, asymptomatic individuals. Like all imaging involving ionizing radiation, CACS should be performed according to the guiding principle of radiation protection: radiation exposure “as low as reasonably achievable” (ALARA principle) while maintaining adequate image quality for the given scenario [3]. Technical improvements in the last decade have enabled significant reductions in radiation dose in cardiac CT angiography (CCTA) [4-6]. However, the acquisition protocol for CACS has not significantly changed, despite advances in the relevant software and hardware. Iterative reconstruction techniques, which have become routine in most centers for CCTA, have variable effects on calcium quantification, often precluding their adoption in CACS [7-9]. Furthermore, standard CACS acquisition protocols recommend maintaining a fixed peak tube voltage of 120kVp to ensure calcium scores according to the Agatston method [10], whereas tube voltages in CCTA acquisitions have steadily decreased. These factors have led to continuous reductions in radiation exposure associated with CCTA, while CACS is still associated with average radiation doses of 1-1.5mSv [3, 10].

Third generation dual-source CT (DSCT) with tin filtration can reduce the radiation dose of low-dose non-contrast enhanced scans [11, 12]. Recently, the potential of CT tin filtration (Sn100kVp) for low voltage CACS has been demonstrated with excellent accuracy and a significant reduction in radiation dose compared to the standard 120kVp acquisition. However, the Sn100kVp acquisition showed a systematic decrease in Agatston scores with consequent changes in patient categorization and cardiac risk classification [13].

Tin filtration results in a harder x-ray spectrum of the Sn100kVp acquisition compared to the standard 120kVp spectrum, as it possesses a slightly higher mean. The resulting reduction in calcium Hounsfield units (HU) values affects the overall calcium Agatston score. Third generation DSCT also supports Iterative Beam Hardening Correction (IBHC), a raw data-based beam hardening correction reconstruction technique. A dedicated spectral IBHC CACS material reconstruction can restore the spectral response of standard 120kVp spectrum, which may enable the derivation of comparable Agatston score values from the Sn100kVp acquisition.

Thus, we sought to investigate the accuracy of CACS using Sn100kVp acquisition with IBHC-based calcium material reconstruction compared to the standard 120kVp protocol.

Material and Methods

Study population

This single-center retrospective study was approved by the local Institutional Review Board and written informed consent was obtained from all patients. The study was performed in compliance with HIPAA regulations. Data of 66 patients who underwent a clinically indicated CACS and a dedicated ECG-triggered 100kVp calcium scan with tin filtration (Sn100kVp) as part of a research study between February and May 2016 were retrospectively analyzed. Exclusion criteria comprised known coronary artery disease (prior percutaneous stent implantation or coronary artery bypass grafting). Furthermore, patients with implanted mechanical prosthetic valves ($n=2$) or cardiac devices ($n=2$) were excluded to prevent imaging artifacts. Thus, a total of 62 patients were included for further analysis.

CT acquisition parameters and image reconstruction

CT acquisition was performed with a 3rd generation DSCT system (SOMATOM Force, Siemens Healthcare, Forchheim, Germany) equipped with a fully integrated circuit detector system (Stellar Infinity, Siemens) and two x-ray tubes (Vectron, Siemens).

Traditional calcium scoring was performed via a prospectively ECG-triggered non-contrast sequential acquisition performed at 40% (HR \geq 80bpm) or 70% (HR $<$ 80bpm) of the cardiac cycle using the following parameters: tube voltage 120kVp; automated tube current modulation (CARE Dose4D, Siemens), reference tube current-time product of 80 mAs, collimation: 44 x 1.2 mm, gantry rotation time 0.25 s, matrix size 512 x 512 pixels.

As a research test, an additional prospectively ECG-triggered non-contrast dual source scan with tin filtration was performed on the scanner by means of custom software. Tin filtration was used on both tubes with a tube voltage of 100kVp (Sn100kVp) triggered at 40% (HR \geq 80bpm) or 70% (HR $<$ 80bpm) of the cardiac cycle with the following scan parameters: automated tube current modulation (CARE Dose4D, Siemens) with a reference tube current of 300mAs/rot, collimation: 42 x 1.2 mm, gantry rotation time 0.25 s.

The standard 120kVp scans were reconstructed with a routine weighted filtered back projection (WFBP) algorithm, using a medium sharp convolution kernel (Qr36), 3.0 mm section thickness, and an increment of 1.5 mm. The Sn100kVp studies were reconstructed using a WFBP algorithm with a dedicated IBHC-based calcium material reconstruction, with a medium sharp convolution kernel (Qr36), 3.0mm section thickness and increment of 1.5mm. Typical

reconstruction field of view (FOV) was 160 x 160mm, depending on patient anatomy, in a 512 x 512 pixel image matrix.

Image analysis of CACS scans

Dedicated post-processing evaluation software (*syngo.via* VB10 Calcium Scoring, Siemens Healthcare, Forchheim, Germany) was used for objective and subjective image analyses. Quantification of coronary artery calcium on non-contrast scans was performed by two independent observers with more than 3 and 5 years of experience in cardiovascular imaging. Both were blinded to patient characteristics and the imaging report. The extent of calcification, defined as a plaque with an area $\geq 1.03\text{mm}^2$, was determined using the Agatston score with a detection threshold of 130 HU [1]. To facilitate observer blinding, the minimum time between the evaluations of calcium on corresponding series was 1 week for both observers. The total Agatston score was recorded and values for both acquisitions were compared. Agatston score categories were as follows: 0, 1-10, 11-100, 101-400, 401-1000, and >1000 [14]. Accordingly, Agatston score percentile-based risk categorization was as follows: 0% (very low), 1-25% (low), 26-50% (mild), 51-75% (moderate), 76-95% (high), and >95% (very high) [15]. Signal and noise were determined by placing a region of interest (1cm^2) in the left ventricle. Consistent placement and size of the region of interest was ensured throughout all examinations. The mean (i.e. signal) and standard deviation (SD; i.e. noise) of HU were recorded and the signal-to-noise ratio (SNR) was calculated by dividing the mean HU by the SD. Observers evaluated subjective image quality based on a 4-point Likert scale: 1=poor, 2=fair, 3=good and 4=excellent. To estimate radiation dose, the volumetric CT dose index (CTDI_{vol}), effective tube current-time product and dose-length-product (DLP) were recorded. Effective radiation dose (ED) was estimated by multiplying the DLP with a standard conversion factor of $0.014\text{mSv/mGy}\cdot\text{cm}$ [16].

Statistical analysis

MedCalc (MedCalc Software, version 15, Ostend, Belgium) and SPSS (SPSS 23.0, IBM, Chicago, USA) were used for statistical analysis. Continuous variables were expressed as mean \pm SD. Normal distribution was assessed using the Kolmogorov-Smirnov test. Differences in patient demographics, characteristics, and CT acquisition parameters of the 120kVp and IBHC Sn100kVp acquisitions were evaluated using the *t*-test for independent samples. A chi-square test was used to identify significant differences between radiation dose estimates as well as objective and subjective image parameters of both acquisition protocols. Agatston scores revealed a highly skewed distribution. Therefore, Agatston scores were computed as medians

and 25th and 75th percentiles and Wilcoxon testing was applied for the comparison of scores. Agatston scores were transformed logarithmically by calculating the natural log of (Agatston score +1) to reduce skewness and because the magnitude of the difference depends on the mean of the Agatston scores. The systematic error and the limits of agreement between the Agatston scores obtained with 120kVp and IBHC Sn100kVp were determined according to the Bland-Altman method [17]. The limits of agreement were calculated to establish a range of values wherein 95% of the differences between the Agatston scores obtained with the two protocols would fall. Pearson's correlation was calculated for IBHC Sn100kVp and 120kVp scans. Agreement of Agatston scores derived from both protocols was compared using Cohen's κ statistic. κ values of 0.81 or more, 0.61-0.80, 0.41-0.60, 0.21-0.40, and less than <0.20 were defined as excellent, good, moderate, and poor test, respectively [18]. Cohen's κ analysis was also used with the same coefficients to determine inter-rater agreement. A two-sided p -value ≤ 0.05 was considered statistically significant.

Results

Study population

Sixty-two patients (56% male) were included in this retrospective single-center study. Mean patient age was 63.9 ± 9.2 years and BMI was 28.1 ± 5.2 kg/m². Patient demographics and baseline characteristics are illustrated in Table 1.

Objective and subjective image quality

Image noise was significantly lower with the 120kVp (mean 17.1 ± 3.9 HU) vs. IBHC Sn100kVp (mean 24.9 ± 3.6 HU, $p < 0.0001$) acquisitions. SNR was significantly higher in 120kVp acquisition (mean 2.8 ± 0.7 HU) compared to IBHC Sn100kVp scans (mean 1.8 ± 0.3 HU, $p < 0.0001$).

In regards to subjective image quality, all acquisitions were considered diagnostic by both observers. For the IBHC Sn100kVp scans, two examinations were rated as fair (both patients with BMI > 35 kg/m²). Two 120kVp cases and three IBHC Sn100kVp cases were classified as good; all other examinations showed excellent image quality. No significant differences were observed in subjective image quality ($p = 0.26$).

Radiation dose estimates

Tube-current-time product was 387.2 ± 128.3 mAs vs. 104.2 ± 46.8 mAs ($p < 0.0001$) for IBHC Sn100kVp vs. 120kVp scans, and CTDI_{vol} was 1.28 ± 1.63 mGy vs. 4.06 ± 1.67 mGy ($p < 0.0001$). DLP

was $13.2 \pm 3.4 \text{ mGy} \cdot \text{cm}$ with IBHC Sn100kVp acquisitions and $59.1 \pm 22.9 \text{ mGy} \cdot \text{cm}$ with the 120kVp acquisitions ($p < 0.0001$). The corresponding ED was significantly lower for IBHC Sn100kVp scans ($0.19 \pm 0.07 \text{ mSv}$) compared to 120kVp acquisitions ($0.83 \pm 0.33 \text{ mSv}$, $p < 0.0001$).

Analysis of CACS scans

Using 120kVp acquisition, calcifications were detected in 50 of 62 patients (81%) and were also correctly identified with IBHC Sn100kVp scans. Furthermore, all patients with an Agatston score of zero ($n=12$) from the standard acquisition had an Agatston score of zero with the IBHC Sn100kVp scans. Agatston scores from the two acquisitions showed excellent correlation ($r=0.99$, $p < 0.0001$). The 120kVp and IBHC Sn100kVp scans yielded the following scores (median [25th and 75th percentile]): 34.1 [2.1, 155.2] and 31.7 [2.3, 157.7]; $p=0.057$. Bland-Altman analysis showed negligible systematic error (D) between the Agatston scores obtained with 120kVp and those obtained with the IBHC Sn100kVp acquisition ($D=102\%$; 95% confidence interval: 94%, 126%), with slightly higher values for the 120kVp protocol compared to the IBHC Sn100kVp scans (Figure 1).

Perfect agreement of Agatston score categorization was shown between the acquisitions, $\kappa=1.00$ (95%CI 1.00-1.00). The corresponding classification to the different Agatston score categories is illustrated in Table 2. No patients were reclassified using IBHC Sn100kVp scans in regards to absolute Agatston score category. Agatston score percentile-based risk categorization showed excellent agreement between IBHC Sn100kVp scans and the standard acquisition ($\kappa=0.99$ [95%CI 0.97-1.00]) (Table 2). One patient (1.6%) was reclassified to the next lowest risk category (high to moderate) (Figure 2).

Inter-observer assessment showed excellent agreement $\kappa=0.95$ (95%CI 0.92-0.98). Representative examples of IBHC Sn100kVp and standard 120kVp scans are shown in Figure 3.

Discussion

Our results demonstrate that CACS with tin filtration using dedicated IBHC calcium material reconstruction showed no significant differences in Agatston scores compared to the standard 120kVp acquisition; there was perfect agreement for Agatston score categorization ($\kappa=1.00$) and nearly perfect agreement for percentile-based cardiac risk categorization ($\kappa=0.99$). CACS with tin filtration using IBHC reconstructions reduces radiation dose by 75% while maintaining Agatston calcium scores. These qualities are desirable for a population-based screening test in a considerable segment of *a priori* healthy, asymptomatic individuals who undergo calcium detection and quantification for the purpose of health maintenance and coronary artery disease prevention.

Our findings in a clinical study population agree with and broaden the findings of McQuiston et al. who used CACS with tin filtration in an anthropomorphic non-moving thorax phantom, demonstrating excellent agreement of calcium quantification using the Agatston method without significant differences in scores using Sn100kVp compared to 120kVp scans [7]. A previous clinical study showed the ability of CACS with tin filtration to significantly reduce radiation dose; however, significant differences in Agatston scores were observed with detrimental effect on cardiac risk stratification [13].

In the present study, Agatston scores showed excellent agreement without significant difference and only a slight underestimation of scores (2%) using the IBHC calcium material reconstruction; furthermore, the cardiac risk reclassification rate was only 1.6%. Previous studies have examined radiation dose reduction in CACS using acquisition protocols with lower tube voltage or tube current [19-21]. They showed excellent correlation ($r=0.99$) and agreement ($\kappa=95-98$) of Agatston scores compared to traditional acquisition methods. However, systematic over- or underestimation of Agatston scores was observed, either requiring adjusted thresholds of 147HU instead of the standard 130HU for calcium quantification or leading to clinically relevant rates of change (up to 7%) in cardiac risk reclassification. Our data suggests that CACS with tin filtration and IBHC reconstruction compares more favorably with traditional CACS acquisitions, without the need for calcium threshold adjustment.

CACS with tin filtration enables a 75% reduction in radiation dose, with a mean effective dose of 0.19mSv in the present study, roughly equivalent to a two-view chest x-ray. This mean effective dose is significantly lower than previously reported radiation values: Hecht et al. (0.37mSv), Dey et al. (1.0mSv), and Nakazato et al. (1.17mSv) using different tube voltages (100kVp vs. 120kVp) or tube current settings (80mAs and 150mAs vs. 180mAs) to reduce radiation dose [20-22]. Marwan et al. reported radiation dose reduction with an effective dose of 0.20mSv; however, in their approach using 100kVp acquisition, Agatston score determination required a threshold adjustment of 147HU [19].

In the present study, the significant reduction in radiation dose obtained by the Sn100kVp scan was associated with an increased image noise compared to the standard 120kVp acquisition. According to current guidelines of the Society of Cardiovascular Computed Tomography for minimizing radiation exposure, CACS should be performed with image noise <23HU [3]. However, this was only achieved in one third of patients using Sn100kVp with IBHC reconstruction. Various iterative reconstruction algorithms have been introduced that show potential in image noise reduction (particularly in low dose acquisitions) compared to standard FBP, which would improve image quality [23, 24]. Accordingly, iterative reconstruction may be a potential target for use in CACS with tin filtration and IBHC reconstruction to reduce image noise, however this hypothesis warrants further investigation.

There are several limitations in the present study that need to be considered. This was a single-center retrospective study with a relatively small patient cohort. Larger studies are necessary to validate our findings. All images were post-processed on the same workstation from one vendor using the manufacturer-specific IBHC calcium material reconstruction. Thus, our results cannot be generalized or adopted to other vendors. Furthermore, a tube voltage of 120kVp and automated tube current modulation with a reference tube current of 80mAs was used in this study as the established, vendor recommended standard protocol. We did not evaluate the effect of radiation dose reduction at 120kVp by decreasing the tube current to achieve the same image noise as in the Sn100kVp study. We did not specifically evaluate the impact of BMI on CACS. However, appropriate patient size cut-off values need to be determined in a future study with a larger cohort.

In conclusion, this study demonstrates the potential feasibility of tin filtration for low-dose CACS with IBHC calcium material reconstruction to restore the fidelity and comparability of calcium values. Compared to standard acquisitions, CACS with tin filtration and IBHC reconstruction showed no significant differences in Agatston scores, with near-perfect agreement in Agatston score categorization and cardiac risk categorization, while significantly decreasing radiation dose.

Disclosures: Dr. Schoepf receives institutional research support from Astellas, Bayer, Bracco, GE, Medrad, and Siemens. Drs. Schoepf, De Cecco, and Varga-Szemes are consultants for Guerbet. Mr. Canstein and Dr. Allmendinger are employees of Siemens Healthcare GmbH. The other authors have no conflict of interest to disclose. Some of the authors of this manuscript are employed by or are consultants for Siemens Healthcare GmbH. The data was analyzed and controlled by authors who are not employed by or a consultant for this industry.

Conflict of interest:

Dr. Schoepf receives institutional research support from Astellas, Bayer, Bracco, GE, Medrad, and Siemens. Drs. Schoepf, De Cecco, and Varga-Szemes are consultants for Guerbet. Mr. Canstein and Dr. Allmendinger are employees of Siemens Healthcare GmbH. The other authors have no conflict of interest to disclose. Some of the authors of this manuscript are employed by or are consultants for Siemens Healthcare GmbH. The data was analyzed and controlled by authors who are not employed by or a consultant for this industry.

References

- [1] A.S. Agatston, W.R. Janowitz, F.J. Hildner, N.R. Zusmer, M. Viamonte, Jr., R. Detrano, Quantification of coronary artery calcium using ultrafast computed tomography, *J Am Coll Cardiol* 15(4) (1990) 827-32.
- [2] R.W. Bauer, C. Thilo, S.A. Chiaramida, T.J. Vogl, P. Costello, U.J. Schoepf, Noncalcified atherosclerotic plaque burden at coronary CT angiography: a better predictor of ischemia at stress myocardial perfusion imaging than calcium score and stenosis severity, *AJR Am J Roentgenol* 193(2) (2009) 410-8.
- [3] S. Voros, J.J. Rivera, D.S. Berman, R. Blankstein, M.J. Budoff, R.C. Cury, M.Y. Desai, D. Dey, S.S. Halliburton, H.S. Hecht, K. Nasir, R.D. Santos, M.D. Shapiro, A.J. Taylor, U.S. Valeti, P.M. Young, G. Weissman, I. Society for Atherosclerosis, I. Prevention Tomographic, C. Prevention, T. Society of Cardiovascular Computed, Guideline for minimizing radiation exposure during acquisition of coronary artery calcium scans with the use of multidetector computed tomography: a report by the Society for Atherosclerosis Imaging and Prevention Tomographic Imaging and Prevention Councils in collaboration with the Society of Cardiovascular Computed Tomography, *J Cardiovasc Comput Tomogr* 5(2) (2011) 75-83.
- [4] M. Renker, L.L. Geyer, A.W. Krazinski, J.R. Silverman, U. Ebersberger, U.J. Schoepf, Iterative image reconstruction: a realistic dose-saving method in cardiac CT imaging?, *Expert Rev Cardiovasc Ther* 11(4) (2013) 403-9.
- [5] W.H. Yin, B. Lu, N. Li, L. Han, Z.H. Hou, R.Z. Wu, Y.J. Wu, H.X. Niu, S.L. Jiang, A.W. Krazinski, U. Ebersberger, F.G. Meinel, U.J. Schoepf, Iterative reconstruction to preserve image quality and diagnostic accuracy at reduced radiation dose in coronary CT angiography: an intraindividual comparison, *JACC Cardiovasc Imaging* 6(12) (2013) 1239-49.
- [6] M. Meyer, H. Haubenreisser, U.J. Schoepf, R. Vliegenthart, C. Leidecker, T. Allmendinger, R. Lehmann, S. Sudarski, M. Borggrefe, S.O. Schoenberg, T. Henzler, Closing in on the K edge: coronary CT angiography at 100, 80, and 70 kV-initial comparison of a second- versus a third-generation dual-source CT system, *Radiology* 273(2) (2014) 373-82.
- [7] A.D. McQuiston, G. Muscogiuri, U.J. Schoepf, F.G. Meinel, C. Canstein, A. Varga-Szemes, P.M. Cannao, J.L. Wichmann, T. Allmendinger, R. Vliegenthart, C.N. De Cecco, Approaches to ultra-low radiation dose coronary artery calcium scoring based on 3rd generation dual-source CT: A phantom study, *Eur J Radiol* 85(1) (2016) 39-47.
- [8] M. Weininger, K.S. Ritz, U.J. Schoepf, T.G. Flohr, R. Vliegenthart, P. Costello, D. Hahn, M. Beisert, Interplatform reproducibility of CT coronary calcium scoring software, *Radiology* 265(1) (2012) 70-7.
- [9] D. Caruso, C.N. De Cecco, U.J. Schoepf, L.M. Felmlly, A. Varga-Szemes, S. Mangold, C. Canstein, T. Allmendinger, S.R. Fuller, A. Laghi, J.L. Wichmann, Correction Factors for CT Coronary Artery Calcium Scoring Using Advanced Modeled Iterative Reconstruction Instead of Filtered Back Projection, *Acad Radiol* 23(12) (2016) 1480-1489.
- [10] B. Szilveszter, H. Elzomor, M. Karolyi, M. Kolossvary, R. Raaijmakers, K. Benke, C. Celeng, A. Bartykowszki, Z. Bagyura, A. Lux, B. Merkely, P. Maurovich-Horvat, The effect of iterative model reconstruction on coronary artery calcium quantification, *Int J Cardiovasc Imaging* 32(1) (2016) 153-60.
- [11] S. Gordic, F. Morsbach, B. Schmidt, T. Allmendinger, T. Flohr, D. Husarik, S. Baumueller, R. Raupach, P. Stolzmann, S. Leschka, T. Frauenfelder, H. Alkadhi, Ultralow-dose chest computed tomography for

pulmonary nodule detection: first performance evaluation of single energy scanning with spectral shaping, *Invest Radiol* 49(7) (2014) 465-73.

[12] H. Haubenreisser, M. Meyer, S. Sudarski, T. Allmendinger, S.O. Schoenberg, T. Henzler, Unenhanced third-generation dual-source chest CT using a tin filter for spectral shaping at 100kVp, *Eur J Radiol* 84(8) (2015) 1608-13.

[13] C. Tesche, C.N. De Cecco, R. Vliegenthart, M.H. Albrecht, A. Varga-Szemes, T.M. Duguay, U. Ebersberger, R.R. Bayer, 2nd, C. Canstein, B. Schmidt, T. Allmendinger, S.E. Litwin, P.B. Morris, T.G. Flohr, E. Hoffmann, U.J. Schoepf, Accuracy and Radiation Dose Reduction Using Low-Voltage Computed Tomography Coronary Artery Calcium Scoring With Tin Filtration, *Am J Cardiol* (2016).

[14] F.Z. Wu, M.T. Wu, 2014 SCCT guidelines for the interpretation and reporting of coronary CT angiography: a report of the Society of Cardiovascular Computed Tomography Guidelines Committee, *J Cardiovasc Comput Tomogr* 9(2) (2015) e3.

[15] R.L. McClelland, H. Chung, R. Detrano, W. Post, R.A. Kronmal, Distribution of coronary artery calcium by race, gender, and age: results from the Multi-Ethnic Study of Atherosclerosis (MESA), *Circulation* 113(1) (2006) 30-7.

[16] J. Hausleiter, T. Meyer, F. Hermann, M. Hadamitzky, M. Krebs, T.C. Gerber, C. McCollough, S. Martinoff, A. Kastrati, A. Schomig, S. Achenbach, Estimated radiation dose associated with cardiac CT angiography, *JAMA* 301(5) (2009) 500-7.

[17] J.M. Bland, D.G. Altman, Statistical methods for assessing agreement between two methods of clinical measurement, *Lancet* 1(8476) (1986) 307-10.

[18] J.R. Landis, G.G. Koch, An application of hierarchical kappa-type statistics in the assessment of majority agreement among multiple observers, *Biometrics* 33(2) (1977) 363-74.

[19] M. Marwan, C. Mettin, T. Pfloderer, M. Seltmann, A. Schuhback, G. Muschiol, D. Ropers, W.G. Daniel, S. Achenbach, Very low-dose coronary artery calcium scanning with high-pitch spiral acquisition mode: comparison between 120-kV and 100-kV tube voltage protocols, *J Cardiovasc Comput Tomogr* 7(1) (2013) 32-8.

[20] H.S. Hecht, M.E. de Siqueira, M. Cham, R. Yip, J. Narula, C. Henschke, D. Yankelevitz, Low- vs. standard-dose coronary artery calcium scanning, *Eur Heart J Cardiovasc Imaging* 16(4) (2015) 358-63.

[21] R. Nakazato, D. Dey, A. Gutstein, L. Le Meunier, V.Y. Cheng, R. Pimentel, W. Paz, S.W. Hayes, L.E. Thomson, J.D. Friedman, D.S. Berman, Coronary artery calcium scoring using a reduced tube voltage and radiation dose protocol with dual-source computed tomography, *J Cardiovasc Comput Tomogr* 3(6) (2009) 394-400.

[22] D. Dey, R. Nakazato, R. Pimentel, W. Paz, S.W. Hayes, J.D. Friedman, V.Y. Cheng, L.E. Thomson, P.J. Slomka, D.S. Berman, Low radiation coronary calcium scoring by dual-source CT with tube current optimization based on patient body size, *J Cardiovasc Comput Tomogr* 6(2) (2012) 113-20.

[23] R.A. Takx, U.J. Schoepf, A. Moscariello, M. Das, G. Rowe, S.O. Schoenberg, C. Fink, T. Henzler, Coronary CT angiography: comparison of a novel iterative reconstruction with filtered back projection for reconstruction of low-dose CT-Initial experience, *Eur J Radiol* 82(2) (2013) 275-80.

[24] L.L. Geyer, U.J. Schoepf, F.G. Meinel, J.W. Nance, Jr., G. Bastarrika, J.A. Leipsic, N.S. Paul, M. Rengo, A. Laghi, C.N. De Cecco, State of the Art: Iterative CT Reconstruction Techniques, *Radiology* 276(2) (2015) 339-57.

Figure legend

Figure 1

Bland-Altman analysis plots comparing mean logarithmically transformed Agatston scores of IBHC Sn100kVp and 120kVp acquisitions with the differences between the two scans (log Agatston score IBHC Sn100kVp – log Agatston score 120kVp).

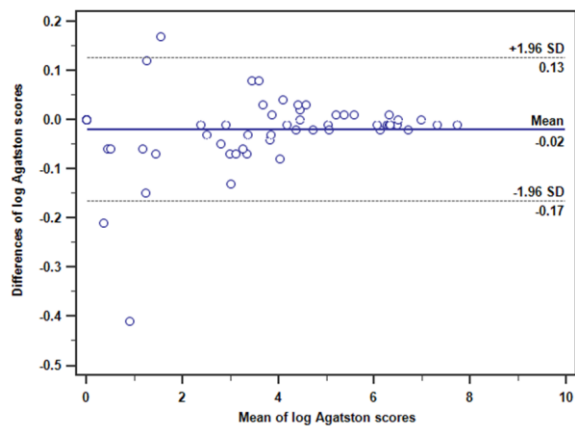


Figure 2

Agatston score categories (A) and Agatston score percentile-based risk categorization (B). Arrows and numbers represent the number of patients reclassified to a different category.

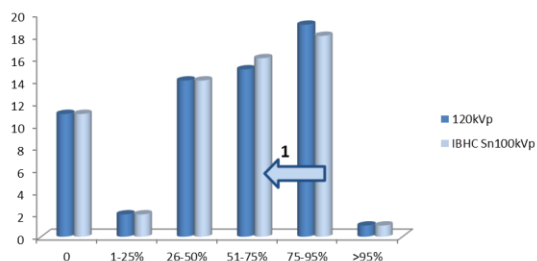
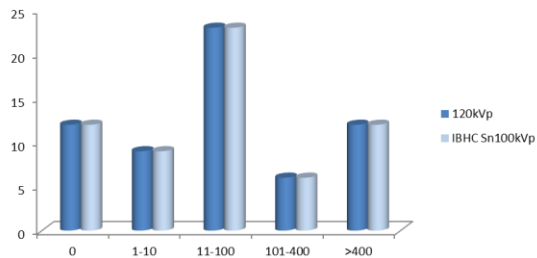
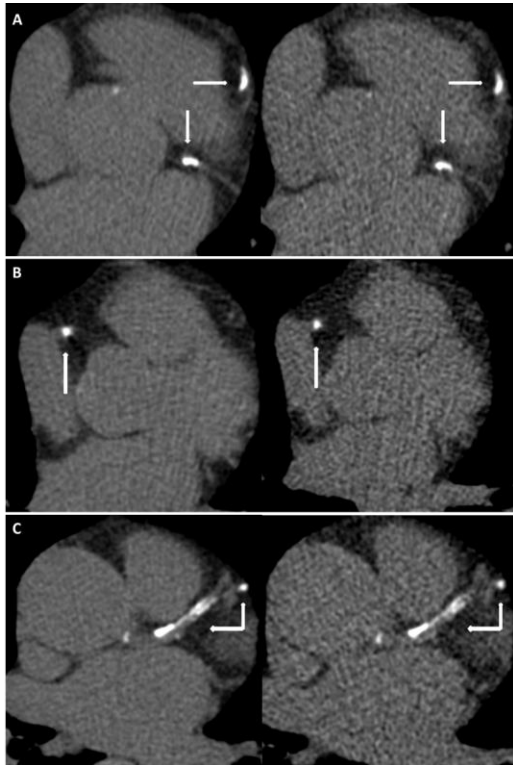


Figure 3

The arrows indicate coronary calcifications with the use of standard 120kVp (left) and IBHC Sn100kVp (right) acquisition. (A) 58-year old man with a BMI of 23.7kg/m² has coronary artery calcium resulting in an Agatston score of 524 with 120kVp and 522 with IBHC Sn100kVp. (B) 53-year old woman with a BMI of 39.7kg/m² has coronary artery calcium resulting in an Agatston score of 38 with both 120kVp and IBHC Sn100kVp. (C) 65-year old woman with a BMI of 29.8kg/m² has coronary artery calcium resulting in an Agatston score of 1254 with 120kVp and 1249 with IBHC Sn100kVp.



Tables

Table 1

Patient characteristics. Total patient cohort ($n=62$).

Age (<i>years</i>)	63.9±9.2
Male sex <i>n</i> (%)	35 (56)
Body-mass-index (<i>kg/m²</i>)	28.1±5.2
Hypertension <i>n</i> (%)	40 (65%)
Diabetes <i>n</i> (%)	11 (18%)
Dyslipidemia <i>n</i> (%)	32 (53%)
Tobacco abuse <i>n</i> (%)	18 (29%)
CAD family history <i>n</i> (%)	14 (24%)

CAD = coronary artery disease. Data presented as mean±standard deviation or numbers with percentages (%).

Table 2

Comparison of Agatston score categories and percentile-based risk categories for the 120kVp and IBHC Sn100kVp acquisition.

Agatston score categories (n=62)							
	0	1-10	11-100	101-400	>400	κ	
120kVp	12	9	23	6	12	1.00 (95%CI 1.00-1.00)	
IBHC Sn100kVp	12	9	23	6	12		
Agatston score percentile-based risk categories (n=62)							
	0%	1-25%	26-50%	51-75%	76-95%	>95%	κ
120kVp	11	2	14	15	19	1	0.99 (95%CI 0.97-1.00)
IBHC Sn100kVp	11	2	14	16	18	1	